ORIGINAL RESEARCH

Bleomycin Induces Drug Efflux in Lungs

A Pitfall for Pharmacological Studies of Pulmonary Fibrosis

Joshua K. Park[1]*, Nathan J. Coffey[1]*, Steven P. Bodine[2], Charles N. Zawatsky[1], Lindsey Jay[1], William A. Gahl[2,3], George Kunos[1], Bernadette R. Gochuico[2], May Christine V. Malicdan[2,3], and Resat Cinar[1]

[1]Laboratory of Physiologic Studies, National Institute on Alcohol Abuse and Alcoholism, National Institutes of Health, Rockville, Maryland; and [2]Section of Human Biochemical Genetics, Medical Genetics Branch, National Human Genome Research Institute, and [3]NIH Undiagnosed Diseases Program and Office of the Clinical Director, National Human Genome Research Institute, National Institutes of Health, Bethesda, Maryland

ORCID ID: 0000-0002-8597-7253 (R.C.).

Abstract

ATP-binding cassette (ABC) transporters are evolutionarily conserved membrane proteins that pump a variety of endogenous substrates across cell membranes. Certain subfamilies are known to interact with pharmaceutical compounds, potentially influencing drug delivery and treatment efficacy. However, the role of drug resistance–associated ABC transporters has not been examined in idiopathic pulmonary fibrosis (IPF) or its animal model: the bleomycin (BLM)-induced murine model. Here, we investigate the expression of two ABC transporters, P-gp (permeability glycoprotein) and BCRP (breast cancer resistance protein), in human IPF lung tissue and two different BLM-induced mouse models of pulmonary fibrosis. We obtained human IPF specimens from patients during lung transplantation and administered BLM to male C57BL/6J mice either by oropharyngeal aspiration (1 U/kg) or subcutaneous osmotic infusion (100 U/kg over 7 d). We report that P-gp and BCRP expression in lungs of patients with IPF was comparable to controls. However, murine lungs expressed increased levels of P-gp and BCRP after oropharyngeal and subcutaneous BLM administration. We localized this upregulation to multiple pulmonary cell types, including alveolar fibroblasts, endothelial cells, and type 2 epithelial cells. Functionally, this effect reduced murine lung exposure to nintedanib, a U.S. Food and Drug Administration–approved IPF therapy known to be a P-gp substrate. The study reveals a discrepancy between IPF pathophysiology and the common animal model of lung fibrosis. BLM-induced drug efflux in the murine lungs may present an uncontrolled confounding variable in the preclinical study of IPF drug candidates, and these findings will facilitate disease model validation and enhance new drug discoveries that will ultimately improve patient outcomes.

Keywords: ATP-binding cassette transporters; idiopathic pulmonary fibrosis; drug resistance; animal models; bleomycin

Idiopathic pulmonary fibrosis (IPF) is a chronic and progressive interstitial lung disease of increasing burden worldwide (1). Despite considerable progress made in understanding IPF pathogenesis, clinical outcomes have yet to improve proportionally. A major challenge to closing this translational gap may be the limitation of animal models recapitulating IPF (2). Traditionally, preclinical studies have focused on the bleomycin (BLM)-induced lung fibrosis mouse model to

(Received in original form April 23, 2018; accepted in final form August 15, 2019)

*These authors contributed equally.

Supported by intramural funds of the National Institute on Alcohol Abuse and Alcoholism, the National Human Genome Research Institute, and the Office of the Director, National Institutes of Health, and the American Thoracic Society Foundation Research Program, and the Hermansky-Pudlak Syndrome Network (R.C.).

Author Contributions: J.K.P. and L.J. performed histology and immunohistochemistry and acquired images. N.J.C. and C.N.Z. performed fluorescent *in situ* hybridization and acquired images. J.K.P. and N.J.C. performed cell-based experiments, contributed to *in vivo* experiments, analyzed data, and wrote the manuscript. W.A.G. and B.R.G. provided clinical samples and participated in manuscript preparation. J.K.P., S.P.B., C.N.Z., L.J., G.K., M.C.V.M., and R.C. contributed to *in vivo* experiments and participated in manuscript preparation. R.C. designed the study, planned *in vitro* and *in vivo* experiments, performed mass spectrometry experiments, analyzed data, interpreted data, and wrote the manuscript.

Correspondence and requests for reprints should be addressed to Resat Cinar, Ph.D., Laboratory of Physiologic Studies, National Institute on Alcohol Abuse and Alcoholism, National Institutes of Health, 5625 Fishers Lane, Room 2S-18, Bethesda, MD 20892-9413. E-mail: resat.cinar@nih.gov.

This article has a related editorial.

This article has a data supplement, which is accessible from this issue's table of contents at www.atsjournals.org.

Am J Respir Cell Mol Biol Vol 62, Iss 2, pp 178–190, Feb 2020

Originally Published in Press as DOI: 10.1165/rcmb.2018-0147OC on August 16, 2019
Internet address: www.atsjournals.org

Clinical Relevance

This article reports a discrepant molecular phenomenon in the widely used animal model of pulmonary fibrosis (PF) that is not observed in human idiopathic pulmonary fibrosis (IPF). Bleomycin (BLM) increases the expression and activity of the ATP-binding cassette transporters, permeability glycoprotein, and breast cancer resistance protein in the murine lungs, which is not observed in human IPF lungs. Because these transporters are known to reduce target exposure to therapeutic compounds, our findings suggest that BLM-induced PF may not be optimal for testing the antifibrotic efficacy of experimental compounds, which are substrates of ATP-binding cassette transporters, intended for IPF therapy. Improved mouse models of IPF are warranted to facilitate the translation of preclinical therapeutics into clinical outcomes.

extrapolate the molecular basis of IPF and predict the clinical efficacy of potential therapeutics (3, 4). However, discrepancies between this animal model and IPF are becoming increasingly apparent. For instance, the histopathologic patterns of BLM-induced lung injury are distinct from those of usual interstitial pneumonia observed in patients (5). In addition, inflammation preceding fibrosis and spontaneous resolution at later time points in the model are inconsistent with IPF at the time of diagnosis. Perhaps the most concerning discrepancy is that drug candidates demonstrating efficacy in this model are too often unsuccessful in clinical trials. Better understanding the limitations of this animal model may improve the translation of preclinical developments into improved patient care.

Mammalian lungs have evolved innate, highly inducible defense mechanisms to respond to insults by exogenous agents. Accordingly, BLM exposure may trigger physiological mechanisms unrelated to IPF pathophysiology. One mechanism by which the lung epithelium guards the alveolar–capillary interface is by expressing active efflux transporters, such as P-gp (permeability glycoprotein/MDR1/*Abcb1*) and BCRP (breast cancer resistance protein/*Abcg2*). Belonging to the ATP-binding cassette (ABC) superfamily of transporters, these integral membrane proteins hydrolyze ATP to eject substrates across the plasma membrane (6). This evolutionarily conserved mechanism restricts the entry of infectious pathogens, particulate matter, and other xenobiotics, protecting host cells from the accumulation of potential toxins (7, 8). However, as a consequence of the broad substrate specificity P-gp and BCRPs for foreign substances, this defense mechanism can also efflux pharmaceutical compounds intended for medical therapy. ABC transporters can therefore interfere with pharmacokinetic parameters, compromise drug delivery, and undermine drug-based treatments. A considerable number of compounds in clinical trials for IPF treatment are known substrates of P-gp, BCRP, or both (Table 1); however, the extent to which ABC transporters affect the study of BLM-induced lung fibrosis remains unknown.

From a clinical standpoint, the overexpression of ABC transporters is associated with multidrug resistance (MDR), which is characterized by cross-resistance against structurally and mechanistically unrelated drugs (9). In thoracic oncology, the high expression of multidrug transporters portends poor response to chemotherapy in both patients with small cell and non–small-cell lung cancer (10–12). P-gp, BCRP, and other MDR-associated transporters can limit intracellular drug concentrations by pumping anticancer agents out of tumor cells, resulting in inadequate target exposure and treatment failure. Evidence indicates that ABC transporters can compromise pharmacotherapy targeting the lungs, but the role of P-gp and BCRP in IPF remains unreported.

To test the hypothesis that P-gp and BCRP are upregulated in IPF and BLM-induced lung fibrosis, we profiled the expression of these transporters in the lungs of patients with IPF and two different BLM-induced mouse models. This article reports that IPF lungs expressed P-gp and BCRP at baseline, constitutive levels, whereas BLM administration to mice either by oropharyngeal (OP) aspiration (OP-bleo) or subcutaneous (SC) osmotic minipump (SC-bleo) upregulated P-gp and BCRP expression in multiple murine pulmonary cell types. Functionally, this upregulation reduced murine lung exposure to nintedanib, an approved treatment for IPF and known P-gp substrate. Our study suggests that BLM introduces an uncontrolled physiological variable confounding preclinical studies on IPF drug candidates.

Methods

Human Lung Tissue

Patients with IPF meeting eligibility criteria (13) provided written informed consent to enroll in protocol 04-HG-0211, "Procurement and Analysis of Specimens from Individuals with Pulmonary Fibrosis," which was approved by the Institutional Review Board of the National Human Genome Research Institute. Fibrotic lung specimens were obtained from three female and three male patients with IPF with an average age of 60 years. Normal lung specimens from anonymous autopsy donors without lung disease were procured within 6 hours of death (National Disease Research Interchange). Lung tissue was procured as previously described (14, 15). Small-cell carcinoma tissue sections (cat. no. T2235152-9) were purchased from BioChain.

Animals

All animal procedures were conducted in accordance with the rules and regulations of the Institutional Animal Care and Use Committee of the National Institutes of Alcohol Abuse and Alcoholism and the National Human Genome Research Institute. Male and female C57BL/6J mice (13 wk old) were purchased from the Jackson Laboratory. Animals were housed individually under a 12-hour light/dark cycle and fed a standard diet, *ad libitum* (Teklad NIH-31; Envigo).

OP Aspiration of BLM

BLM (Hospira) was administered as previously described (16, 17). BLM (1 U/kg) was delivered into the oropharynx at a volume of 100 μl/50 g body weight using a 100-μl pipette. Saline was used as the vehicle treatment for control groups.

SC Osmotic Delivery of BLM

This protocol was approved by the National Human Genome Research Institute and National Institutes of Alcohol Abuse and

Table 1. Interactions with P-gp and BCRP for Approved and Study Drugs for Idiopathic Pulmonary Fibrosis*

Status	Drug	P-gp	BCRP
Approved			
	Pirfenidone	Inhibitor	—
	Nintedanib	Substrate	—
Phase 3			
	Ambrisentan†	Substrate	—
	Bosentan†	Substrate	—
	Warfarin†	Inhibitor, substrate	—
	Imatinib†	Substrate	Substrate
	Sildenafil†	Inhibitor	—
	IFN-γ†	Inducer	—
	Trimethoprim‡§	Inhibitor, inducer	—
	NAC†	—	—
Phase 2			
	Losartan	Substrate, inhibitor	—
	Prednisone‡	Substrate, inhibitor	—
	Macitentan†	Inducer	—
	BG00011 (STX100)	—	—
	PRM-151	—	—
	SAR156597	—	—
	TD139	—	—
	Treprostinil	—	—
	GLPG1690	—	—
	Tetrathiomolybdate	—	—
	Zileuton	—	—
	Etanercept†	—	—
	BMS-986020†	—	—
	KD025‡	—	—
	CC-90001‡	—	—
	Compound 36 (GBT440)†	—	—
	PBI-4050	—	—
	Tipelukast‡	—	—
	Octreotide	—	—
	Azathioprine‡	—	—
	QAX576	—	—
Phase 1			
	Dasatanib	Substrate, inhibitor	—
	Vismodegib§	Substrate	Inhibitor
	Sirolimus	Inhibitor, inducer	—
	Quercetin‡§	Inhibitor	Inhibitor
	IW001	—	—
	Nandrolone decanoate	—	—
	Omipalisib (GSK2126458)	—	—
	GSK3008348	—	—
	Tanzisertib (CC-930)†	—	—
Preclinical			
	Colchicine	Substrate, inhibitor, inducer	—
	Felodipine	Inhibitor	—
	Atorvastatin	Inhibitor	—
	Protectin DX	—	—
	Everolimus	—	—

Definition of abbreviations: BCRP = breast cancer resistance protein; NAC = *N*-acetylcysteine; P-gp = permeability glycoprotein.
*This table was compiled using DrugBank 5.0 (www.drugbank.ca), which is a comprehensive drug database supported by the Canadian Institutes of Health Research (40). This is not a list of all drugs in development as therapy for idiopathic pulmonary fibrosis.
†Negative results.
‡Currently recruiting participants (www.clinicaltrials.gov).
§In a combination strategy.

Alcoholism Animal Care and Use Committees, under protocols G-14–3 and LPS-GK1, respectively. Methods for SC-bleo administration were modified from Lee and colleagues (18) and are described in the data supplement.

Lung Function Measurements

Respiratory system mechanics measurements were performed using the flexiVent FX system (SCIREQ Inc.), which is equipped with an FX1 module and negative-pressure forced expiration extension for mice. FlexiWare v7.2 software was used for operating the system. Forced oscillation techniques and forced expiration measurements were conducted as described previously (19, 20) and detailed in the data supplement.

Hydroxyproline Measurement by Liquid Chromatography–Tandem Mass Spectrometry

Lung fibrosis was quantified by measuring hydroxyproline (Hyp) content of lung extracts using liquid chromatography–tandem mass spectrometry, as described previously (16), with slight modifications as described in the data supplement.

LPS-induced Acute Lung Injury

To induce acute lung injury, 16-week-old mice received a single OP instillation of LPS (50 μg/mouse) as described previously (21). LPS was dissolved in sterile saline and administered as 50 μg/mouse in 40 μl after anesthesia induced by ketamine/xylazine. The control group received sterile saline. The mice were studied 1 and 7 days after LPS instillation.

Statistical Analysis

Values are reported as mean (±SEM). Data were analyzed with unpaired two-tailed Student's *t* test or one-way ANOVA using GraphPad Prism 7 (GraphPad Software Inc.). The criterion for significance was *P* less than 0.05.

Additional methods and details not listed here are provided in the data supplement.

Results

Prolonged Activation Pattern of Drug Efflux Transporter Genes in Response to Administration of BLM via Different Delivery Routes in Mouse Models of Pulmonary Fibrosis

BLM-induced pulmonary fibrosis develops primarily in stages: initial tissue injury is followed by lung inflammation and then fibrosis. The time course of inflammation and fibrosis varies in BLM-induced PF

murine models with route of BLM administration. Accordingly, gene expression status of ABC transporters throughout lung fibrosis development in mice was compared for two different BLM delivery routes: either single administration by OP instillation (1 U/kg) or continuous SC delivery by osmotic minipump for 7 days (100 U/kg). Male mice used for this study were age- and weight-matched as 13 weeks old and between 25 and 28 g. OP and SC BLM administration resulted in a similar trend in body weight reduction until Day 12, then body weights gradually recovered to starting weights by Day 35 (Figure 1A). Although BLM delivered through intratracheal or OP routes induces patchy and heterogeneous fibrosis, we chose to dedicate different lung lobes of the same mice for homogenous representation of pathology, and to minimize the number of animals used in the study, we followed a strategy for data collection from different lung lobes (16), where we found good correlation between Ashcroft scoring, hydroxyproline content, and gene expression pattern of fibrogenic markers. The whole left lung was used for hydroxyproline analysis, whereas the upper and lower lobes of the right lung were used for histological studies, such as Masson's trichrome, as well as for fluorescent *in situ* hybridization; the right middle lobe was used for gene expression analysis. Lung function measurements by flexiVent were also employed, providing physiological status of the whole lung. To observe pulmonary fibrosis (PF) development progress in different BLM delivery routes, multiple parameters were analyzed on Days 7, 14, 28, and 42 after initial BLM delivery in both OP-bleo and SC-bleo models.

The wet weight of the left lung significantly increased by 7 days after BLM instillation, then remained elevated in OP-bleo (1 U/kg), whereas the same metric did not significantly increase until Day 14 in SC-bleo (100 U/kg) (Figure 1B). Fibrosis, as represented by hydroxyproline content, was quantifiable in the OP model on Day 7, progressively increased until Day 28, then slightly decreased by Day 42 (Figure 1C). This trend might be explained by the fibrosis resolution in OP-bleo. In the SC model, hydroxyproline content was unaffected at Day 7, then slightly increased by Day 14. Peak hydroxyproline levels were observed on Day 28 and remained at peak levels on Day 42 (Figure 1C). The delayed fibrosis development observed in the SC-bleo model may be explained by the continuous and sustained infusion of systemic delivery. Gene expression of the fibrogenic markers, *Col1a* (Collagen 1a) and *Fn1* (fibronectin), in the OP-bleo model were significantly increased on Day 7, peaked at Day 14, then returned to the normal range on Day 42 (Figure 1D). The expression of the same genes in SC-bleo remained at baseline until a significant increase was measured on Day 14. In the SC-bleo model, *Fn1* expression peaked on Day 14, then declined to just above baseline by Day 42, whereas Col1a measurement peaked on Day 28, then returned to baseline by Day 42 (Figure 1C). Both models had peak left lung weight measurements on Day 14, and comparable left lung weights on Days 28 and 42, however. Because hydroxyproline levels peaked at Day 28 after BLM then remained high at Day 42, lung function was explored at these time points. OP-bleo and SC-bleo caused a comparable decline at each time point in pulmonary function, as measured by pressure–volume curve (Figure 1E), lung tissue elastance (Figure 1F), and tissue damping (Figure 1G). More severe lung function was observed on Day 28, and was slightly recovered on Day 42. All these outcomes agree with each other and suggest that both OP-bleo and SC-bleo induced comparable PF and peaked at Day 28 after BLM. Importantly, both OP-bleo and SC-bleo administration significantly elevated the gene expression of *Abcb1b* and *Abcg2*, which encode P-gp and BCRP, respectively. Both genes were significantly elevated by Day 14 in the OP model, and remained elevated throughout the fibroproliferative process up until Day 28 (Figure 1H). Both genes showed a significant increase in expression on Day 14 in the SC model, and remained significantly elevated on Day 28, returning to baseline by Day 42 (Figure 1I).

P-gp and BCRP Protein Levels in Lung Tissue Are Elevated with BLM, but Not in Human IPF

Upon finding that OP-bleo and SC-bleo are associated with robust upregulation of *Abcb1b* and *Abcg2* expression (Figures 1H and 1I), the question was raised whether this difference in gene expression is observed at the protein level. Both OP- and SC-bleo mouse lungs showed quantifiable fibrosis biochemically (Figure 1B) and histologically (Figure 2A). P-gp and BCRP protein levels were assessed in OP- and SC-bleo mice using immunohistochemical staining. The lungs of saline-treated control mice expressed baseline levels of both transporters (Figures 2C and 2E), whereas those of OP-bleo and SC-bleo mice were associated with a remarkable increase in both P-gp and BCRP on Days 14, 28, and 42 (Figures 2 and Figure E1 in the data supplement).

A subsequent question arose as to whether the upregulation of P-gp and BCRP genes and proteins observed in OP-bleo and SC-bleo models reflects conditions in human IPF. Paraffin-embedded lung sections were obtained from patients with IPF and control subjects without known lung disease. Because the upregulation of drug efflux transporters is well documented in small-cell carcinoma (SCC) (10, 11, 22), human lung sections of SCC were concurrently analyzed as a positive control of methods and reagents. Although P-gp and BCRP were overexpressed in SCC as expected, healthy human lung minimally expressed these proteins (Figures 2D and 2F). Notably, IPF lungs presented with significant collagen deposition and fibrosis (Figure 2B), yet the marginal level of expression of these transporters was indistinguishable from that of control lungs. These results indicate that human IPF is not associated with the upregulation of P-gp and BCRP observed in the OP-bleo and SC-bleo models, despite comparable histological presentation of fibrosis (Figures 2A and 2B).

P-gp and BCRP Express in Multiple Cell Types in Lung upon BLM Challenge

The immunohistochemical staining for P-gp and BCRP in mouse lung tissue suggested the involvement of multiple cell types in upregulation of these proteins (Figures 2C and 2D). To identify the cell types expressing *Abcb1b* and *Abcg2*, fluorescent RNA *in situ* hybridization was performed on formalin-fixed, paraffin-embedded lung sections from 14 days after OP-bleo and SC-bleo along with control mice. Expression of *Abcb1b* and *Abcg2* was observed in macrophages (*Cd68*), alveolar type 2 epithelial (ATII) cells (*Sftpc*), endothelial cells (*Pecam1*), pericytes (*Cspg4*), and collagen-producing cells, such as fibroblasts and myofibroblasts (*Col1a1*) (Figures 3 and 4). These results corroborate those of previous studies, which

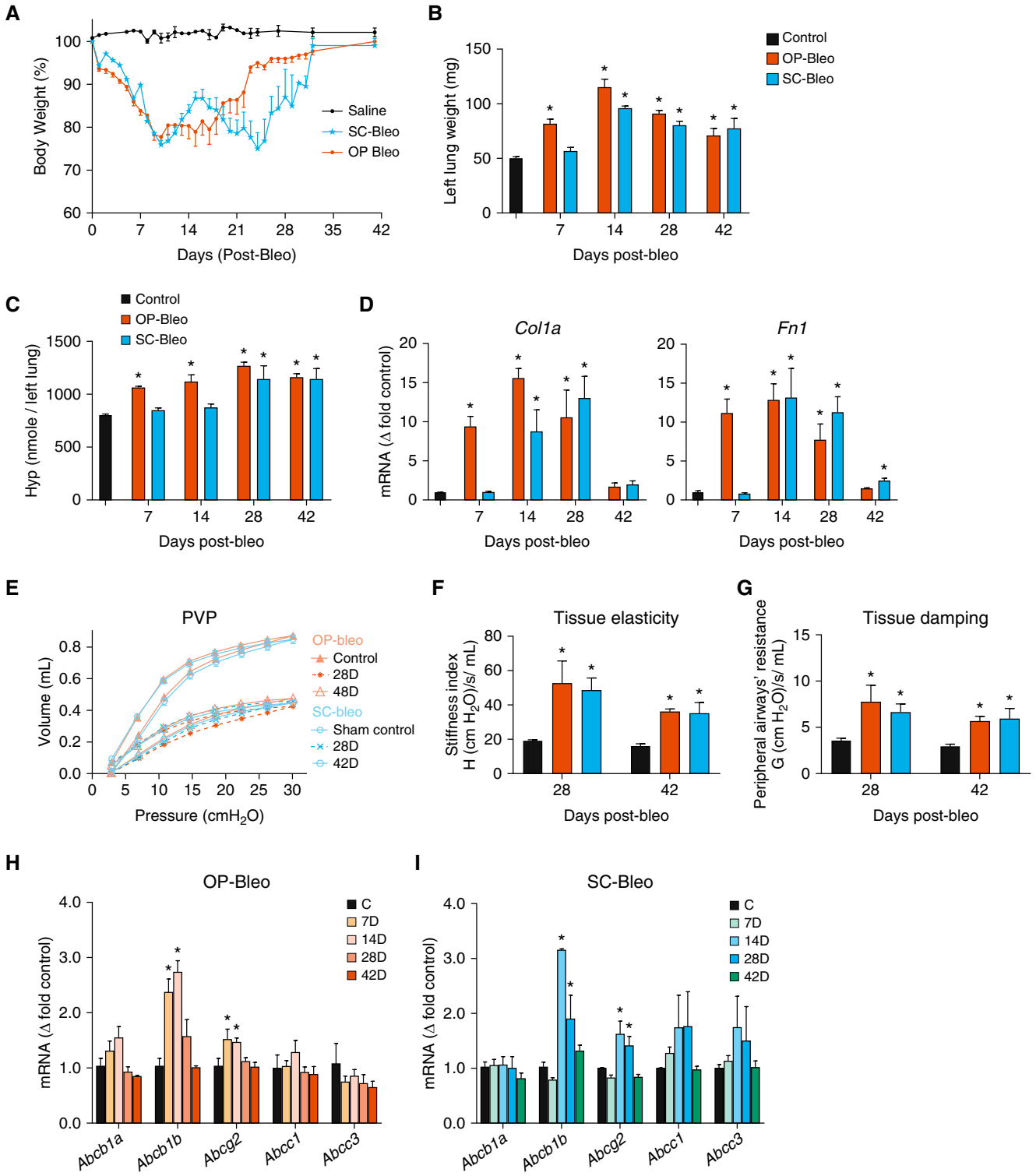

Figure 1. Both oropharyngeal bleomycin (OP-bleo) and subcutaneous bleomycin (SC-bleo) induce comparable pulmonary fibrosis with upregulating P-gp (permeability glycoprotein) and BCRP (breast cancer resistance protein) gene expression. (*A*) Percent initial body weight. Initial average body weight was 26 ± 2 g for each group. (*B*) Wet weight of the left lung was recorded after OP-bleo or SC-bleo. (*C*) Hydroxyproline (Hyp) content of the left lung was measured via liquid chromatography–tandem mass spectrometry (LC-MS/MS) after OP-bleo or SC-bleo. (*D*) Gene expression profiling of fibrosis markers. (*E*) Pressure–volume curve, (*F*) tissue elasticity, (*G*) tissue damping, as a measure of lung function obtained by flexiVent. Gene expression of drug efflux–associated ATP-binding cassette (ABC) transporters after (*H*) OP-bleo or (*I*) SC-bleo. $n = 5$ mice per group for control and 6 mice per OP-bleo group, and 5 mice per SC-bleo group. $^*P < 0.05$ indicates significant difference from control group. PVP = pressure–volume curve.

demonstrated that *Abcb1b* and *Abcg2* are expressed in many cell types in the lung, including ATII cells, macrophages, endothelial cells, and fibroblasts (23).

Tracheal BLM Enhances Drug Efflux in Murine Lungs and Reduces Target Exposure of the U.S. Food and Drug Administration–approved IPF Medication, Nintedanib, a P-gp Substrate

Most therapeutic drugs reach their target organ via the systemic route and circulation; therefore, one of the most critical cell types for excluding xenobiotics from a target organ is endothelial cells, as demonstrated by the blood–brain barrier. In the current study, BLM increased expression of P-gp and BCRP not only in endothelial cells, but also in fibroblasts, macrophages, ATII cells, and pericytes, which have critical roles in the fibroproliferative process in lung tissue (Figure 3 and 4). Indeed, most of the therapeutic drugs target a protein in one or many of those cells. An increase in P-gp expression, however, does not necessarily lead to enhanced drug efflux activity, which may be measured using a P-gp substrate (24). Nintedanib is a U.S. Food and Drug Administration–approved IPF therapy in clinical use, as well as a substrate of P-gp. To understand the functional consequence of the observed diverse upregulation of P-gp and BCRP, blood plasma and lung tissue levels of nintedanib were compared for OP-bleo, SC-bleo, and control mice killed on study Days 14, 28, and 42, 1 hour after administration of 30 mg/kg nintedanib. Plasma and lung tissue nintedanib concentrations were measured using liquid chromatography–tandem mass spectrometry (Figure 5).

Although plasma nintedanib levels were similar in OP-bleo mice and controls at each time point (Figure 5A), lung exposure to nintedanib was dramatically reduced on Days 14 and 28, respectively, measuring 6% (376 ng/g) and 5.3% (298 ng/g) compared with control mice (5,547 ng/g) (Figure 5B). Surprisingly, in SC-bleo mice, oral bioavailability of nintedanib was diminished such that plasma exposure dropped to 320 ng/ml (12% of control) and 71 ng/ml (3% of control) on Days 14 and 28, respectively. Accordingly, lung nintedanib exposure was also significantly reduced at Days 14 and 28 in SC-bleo compared with healthy controls. In both models, lung nintedanib exposure returned to control levels by Day 42 (Figure 5B). This normalization of P-gp activity corroborates our observation of normalized *Abcb1b* gene expression at Day 42 (Figure 1H).

Nintedanib Failed as an Antifibrotic Agent in the OP-Bleo Model due to Lack of Lung Exposure

The 20-fold reduction in nintedanib lung exposure observed in this study indicates a significant alteration in the pharmacokinetic/pharmacodynamic (PK/PD) relationship of nintedanib in OP-bleo mice, as compared with healthy controls. Therefore, nintedanib efficacy was tested in the OP-bleo model. Mice were treated with nintedanib between Days 14 and 28, times when fibrosis progressed and peaked in a study using an intranasal BLM-induced model for testing nintedanib efficacy via daily oral administration of a 30 mg/kg dose; under these conditions, the treatment was somewhat efficacious in female mice (25). In the current study, nintedanib (30 mg/kg) did not effectively reduce fibrosis or restore decreased lung function (Figure 6).

Lower Dose of OP-Bleo Could Generate Lower-Grade Fibrosis while Still Increasing P-gp Activity

The OP-bleo–induced pulmonary fibrosis model in mice is endorsed as a standard model for efficacy studies by the American Thoracic Society (2). As this study's findings may raise serious concerns regarding use of the OP-bleo model in preclinical efficacy studies for P-gp and BCRP substrates, a lower BLM dose was tested to observe whether fibrosis could be induced without upregulation of P-gp and BCRP. A single BLM dose of 0.3 U/kg was administered via OP delivery. The exposed mice developed significantly lower-grade fibrosis (Figure E2B), as measured by hydroxyproline, when compared with mice exposed to 1 U/kg OP-BLM (Figure 1B); however, P-gp and BCRP gene and protein expression were still upregulated. (Figures E2C and E2D). Furthermore, 0.3 U/kg BLM also prevented lung exposure of nintedanib, just as did 1 U/kg of BLM at Days 14 and 28 after BLM (Figure E2E), with comparable serum nintedanib levels (Figure E2F). These findings suggest that lower BLM doses could still compromise the pulmonary fibrosis model for testing substrates of P-gp and BCRP transporters.

Op-Bleo Induced P-gp in Lungs of Male Mice More Dramatically than in Female Mice

The prevalence of IPF is higher in men than in women (26). Besides, preclinical research on PF is mostly conducted in male mice. It is also known that BLM-induced pulmonary fibrosis is less pronounced in female compared with male mice (27). We tested whether there is a similar sex-dependent dimorphism in the ability of BLM to upregulate P-gp in the lung. OP-bleo (1 U/kg) induced more weight loss (Figure E3A) and fibrosis (Figure E3B) in male mice than in female mice. Importantly, OP-bleo induced significantly greater P-gp protein expression in male mice than in female mice (Figure E3C).

Age- and Dose-Dependent Variable Effects of BLM via SC-Osmotic Pump Delivery

A 100-U/kg dose of SC-bleo induced comparable lung fibrosis as that observed with 1 U/kg OP-bleo (Figure 1); however, it still induces upregulation of P-gp and BCRP in the lung. SC-bleo provides continuous release of BLM, inducing delayed injury and fibrosis at Day 14 (Figures 1B–1D). Accordingly, it was hypothesized that sustained release of BLM would allow for dose titration, therefore optimizing the BLM mouse model by avoiding the robust acute injury and cell damage generated by OP-bleo. SC-bleo doses of 60 and 100 U/kg were tested in 13-week-old mice with an average initial body weight of 26 g; however, the 60-U/kg dose of BLM did not induce fibrosis (Figure E4A). Because the dose is given systemically as U/kg, the body weight of mice would have an impact on the systemic dose, which could also change according to the age of the mice (Figure E4A). Therefore, 100 U/kg was tested on 24-week-old mice with an average initial body weight of 35 g. A dose of 100 U/kg induced more fibrosis in these mice (Figure E4A), and also caused very severe body weight loss (Figure E4B).

SC-bleo Induces Expression of P-gp in Small Intestine

Earlier studies showed cytotoxicity and inflammatory effects of systemic BLM in

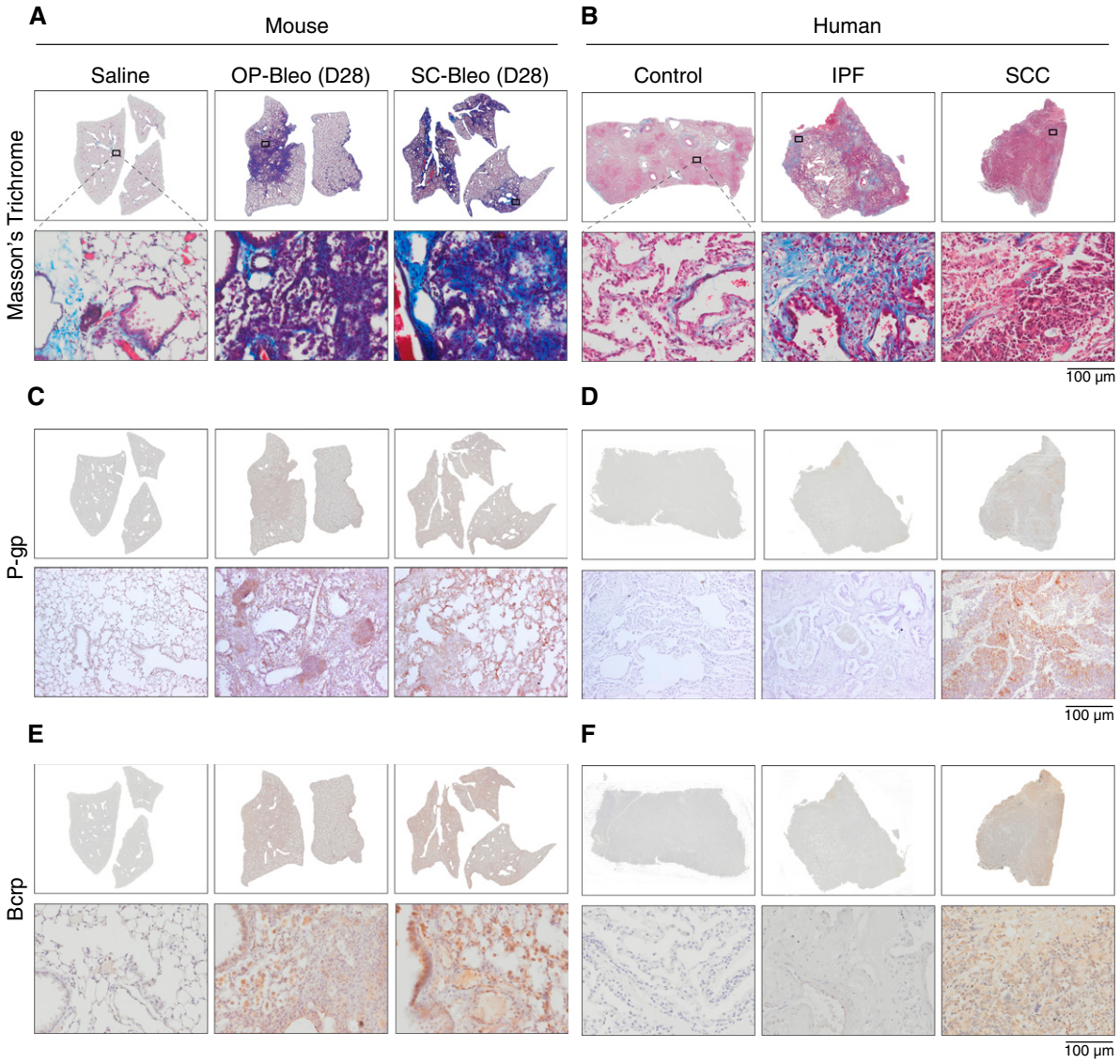

Figure 2. P-gp and BCRP protein levels are elevated in the bleo models but not in human idiopathic pulmonary fibrosis (IPF). Mouse and human lung sections were stained with Masson's trichrome staining. Fibrosis was present in both (*A*) OP-bleo and SC-bleo models, as well as (*B*) human IPF. Immunohistochemical staining revealed elevated P-gp protein levels in (*C*) OP-bleo and in SC-bleo but not in (*D*) human IPF. Similarly, BCRP protein was increased in (*E*) OP-bleo and in SC-bleo but not in (*F*) human IPF. Small-cell carcinoma (SCC) sections had substantial P-gp and BCRP expression, as expected. $n = 4$ mice per control group and 5 mice per OP-bleo and SC-bleo groups. $n = 4$ for nonfibrotic human control group, 6 for patients with IPF, 2 per SCC group. Scale bars: 100 μm.

small intestine (28). P-gp is functionally expressed in small intestines, which affects the absorption and oral bioavailability of its substrates. Because nintedanib absorption was dramatically diminished in mice treated with SC-bleo at 14 days (Figure 5), we explored whether this may be related to a parallel increase in BLM-induced overexpression of P-gp in small intestine. Indeed, SC-bleo (100 U/kg) significantly increased expression of P-gp in small intestine (Figure E5).

Effect of LPS-induced Lung Injury on Efflux Pump Transporter in the Lung

OP-bleo induced overexpression and function of P-gp and BCRP in early inflammatory stages (Figure 1), in which robust injury and inflammation accompanied the disease initiation and progression. This brings up the intriguing possibility that this effect might be limited to the BLM-induced injury, or could also be observed in other lung injury models. To test this, we employed the commonly used LPS-induced lung injury model by OP instillation. We investigated the effect on the LPS model 1 and 7 days after instillation, as it is known that acute lung injury can be seen at 1 day and fibroproliferative responses could be observed at the 7 day time point. LPS dramatically increased inflammatory markers of chemokines and cytokines at 1 day after LPS (Figure 7A), but fibrogenic markers increased only at the 7-day time point (Figure 7B). Although, fibrogenic

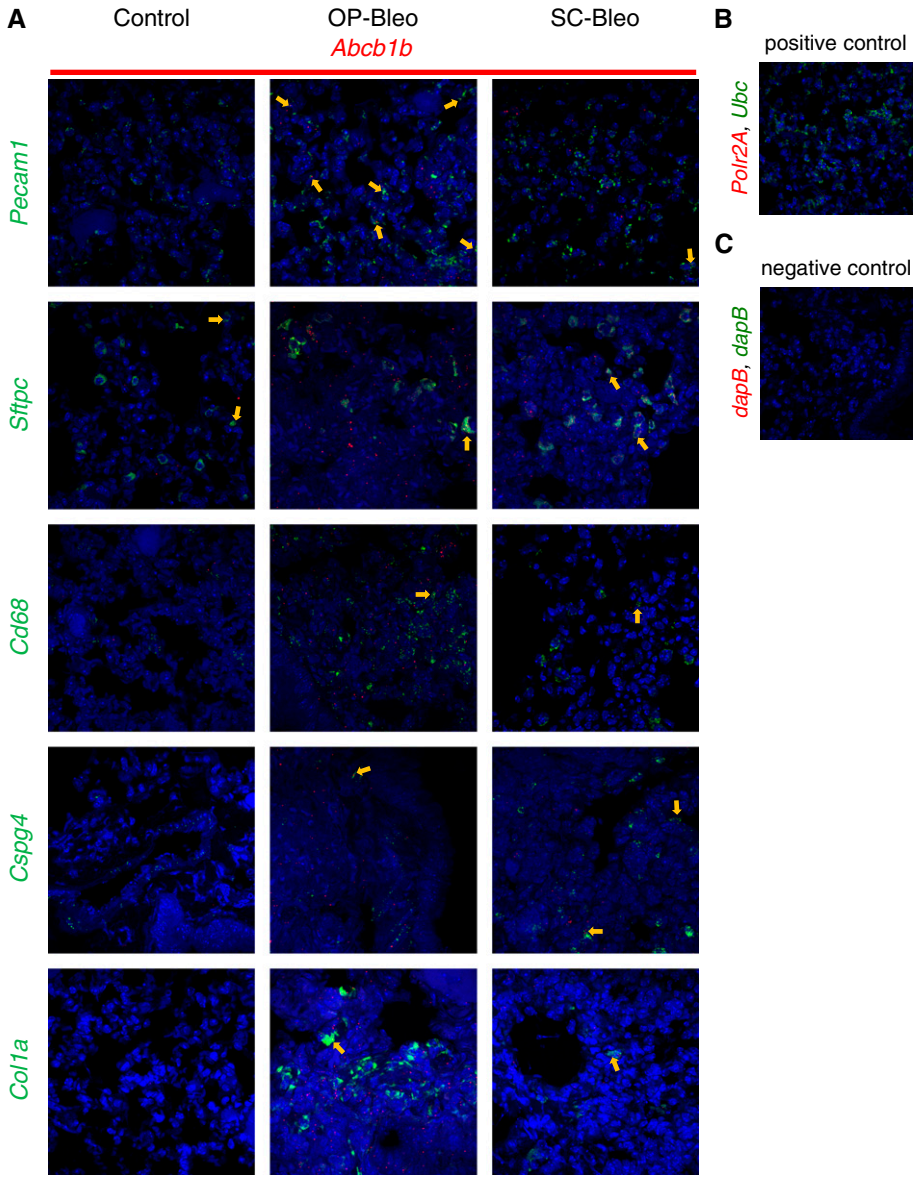

Figure 3. Localization of *Abcb1b* with cell types in the lung. Fluorescent *in situ* hybridization (FISH) was performed with the RNAscope Multiplex Fluorescent Kit V2 on formalin fixed paraffin embedded (FFPE) lung tissue sections from 14-day OP-bleo SC-bleo and control mice. (*A*) FISH detected localization of *Abcb1b* on cells positive for *Cd68* (macrophages), *Sftpc* (alveolar type II epithelial cells), *Pecam1* (endothelial cells), *Col1a1* (collagen-producing cells, such as fibroblasts and myofibroblasts), and *Cspg4* (pericytes). Arrows point out colocalizations. (*B*) FFPE lung tissue RNA quality was assessed using housekeeping genes *Polr2a* (low-expressed gene) and *Ubc* (high-expressed gene) as positive controls. (*C*) FISH nonspecific background staining was assessed using the bacterial gene *dapB* as a negative control. $n = 3$ per group.

markers were significantly increased, hydroxyproline levels were not (Figure 7C). LPS increased only *Abcb1b* gene expression levels at 1 day after LPS, then expression levels returned to the normal range at 7 days after LPS (Figure 7D). On the other hand, protein levels of P-gp increased at 1 day after LPS and then remained elevated by 7 days after LPS (Figure 7E). We did not observe any changes in levels of gene and protein expression of BCRP (Figures 7D and 7E). These data suggest that acute lung injury, which accompanies severe inflammation, could also upregulate P-gp transporter. Inflammatory signals and cellular pathways involved are different between LPS- and BLM-induced lung injury. LPS injury caused a limited and shorter effect, whereas BLM caused long-lasting and much more robust changes in ABC transporter functions.

Discussion

Several IPF drug candidates are known to be substrates of the ABC transporters, P-gp and BCRP (Table 1); however, it is not known whether ABC transporters are dysregulated in IPF pathogenesis or in IPF mouse models. This study tested the hypothesis that either OP- or SC-BLM induced the upregulation of multidrug ABC transporters in the murine lungs. Using molecular and biochemical tools, we detected P-gp and BCRP upregulation at both transcriptional and protein levels in multiple pulmonary cell types of bleo-challenged mice. This upregulation of efflux transporters reduced murine lung exposure to nintedanib, an approved IPF medication, suggesting functional consequences on the pharmacokinetic parameters of substrate compounds. In lung tissue from patients with IPF, we detected only baseline levels of P-gp and BCRP expression, revealing a previously unknown discrepancy between human IPF and the bleo-induced model. This study provides the first evidence of drug efflux–associated ABC transporter dysregulation in mice with pulmonary fibrosis induced by BLM exposure, and these results have implications for preclinical trials investigating treatment for fibrotic lung disease.

OP-bleo delivery to mice is the most widely used and formally recommended method for modeling IPF *in vivo* (2). However, our findings suggest that BLM introduced an uncontrolled physiological variable in mice that may confound preclinical studies using this model. Previous studies have reported that cytotoxic drugs can induce the upregulation of ABC transporters, which, in turn, interfere with drug delivery via efflux of pharmaceutical compounds and reduced target exposure. These reports are consistent with our findings that BLM upregulates P-gp and BCRP in murine lungs, which reduces lung exposure to nintedanib, a P-gp substrate. To what extent this experimental artifact has affected prior studies on IPF remains unknown, but it may have led to the misinterpretation of preclinical trial results, whereby a lack of target exposure was

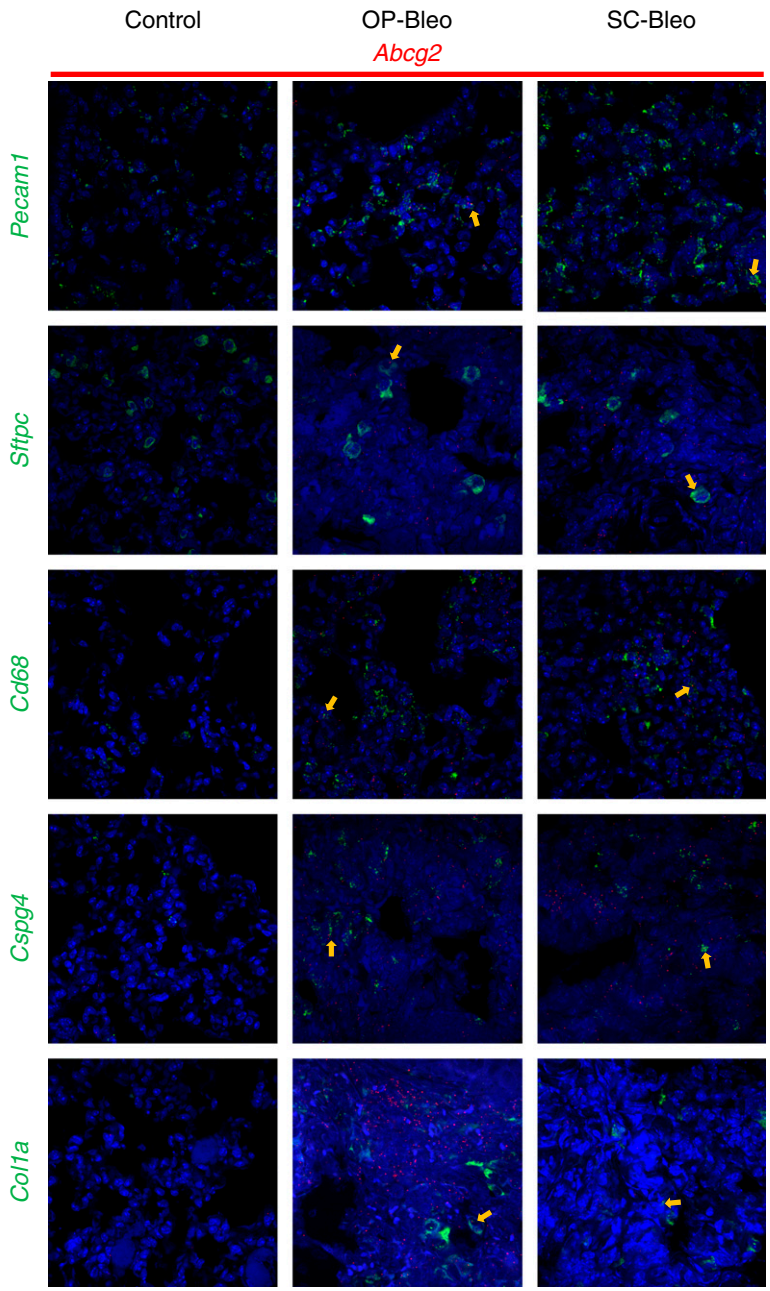

Figure 4. Localization of *Abcg2* with cell types in the lung. FISH was performed with the RNAscope Multiplex Fluorescent Kit V2 on FFPE lung tissue sections from 14-day OP-bleo, SC-bleo, and control mice. FISH detected localization of *Abcg2* on cells positive for *Cd68*, *Sftpc*, *Pecam1*, *Col1a1*, and *Cspg4*. $n = 3$ per group. Arrows point out colocalizations.

misinterpreted as a lack of efficacy, misleading investigators to lose faith in the biological target or lead compound, and, ultimately, false-negative results. We speculate that drug compounds targeting the pulmonary cell types we highlighted may especially demonstrate a multidrug-resistant phenotype like that of chemoresistant cancer cells. This is clinically relevant, as a lack of efficacy in animal models often prevents testing in clinical trials and terminates the development of legitimate drug candidates. Therefore, identifying former IPF drug candidates that are P-gp or BCRP substrates and retesting their antifibrotic efficacy in nonbleo animal models may be warranted. This strategy may be particularly promising for compounds, the biological target of which passes genetic validation *in vivo*.

During clinical development, understanding the PK/PD properties of a proposed drug is essential for planning dosing regimens used in clinical trials. If human data are not available, preclinical animal data become critical for extrapolating doses for phase 1 and 2 trials. Proper drug dosing is important not only for optimizing clinical efficacy, but also for preventing adverse effects. In the context of our findings, an IPF drug candidate may have failed in phase 1 trials due to toxicity if the dosing regimen was extrapolated from the bleo-induced model. Nintedanib was already in clinical development with a known PK/PD relationship in humans, providing an estimate for dosing purposes without relying on data from bleo-induced mice. Fortunately, it also showed preclinical efficacy in intranasal BLM-challenged female mice (25). It is known that the fibrotic response to BLM challenge could be influenced by sex, as female mice are less susceptible to the fibroproliferative effects of BLM (27). Here, we showed that female mice are also less prone than male mice to BLM induction of P-gp in the lungs (Figure E3C), which might explain the conflicting findings regarding the preclinical antifibrotic efficacy of nintedanib (25) (Figure 6). For example, if the preclinical testing had been conducted in either of the models used in this study in male mice, nintedanib may have never reached clinical trials for IPF. From a drug development standpoint, we underscore the importance of recognizing drug interactions with P-gp and BCRP at the earlier stages in the process.

Because the OP-bleo model exhibited P-gp and BCRP upregulation, we explored the possibility of delivering BLM subcutaneously as a potential alternative to OP BLM-induced models. SC-bleo presented comparable levels of fibrosis at 100 U/kg and caused a more gradual, homogenous distribution of BLM compared with the focally high doses caused by OP-bleo instillation. Notably, the SC model produced fibrotic lesion patterns at subpleural and perivascular sites, as reported previously (29–31), which better approximates the histological patterns of human IPF (32, 33). However, SC-bleo significantly affected the absorption and oral bioavailability of nintedanib (Figure 5).

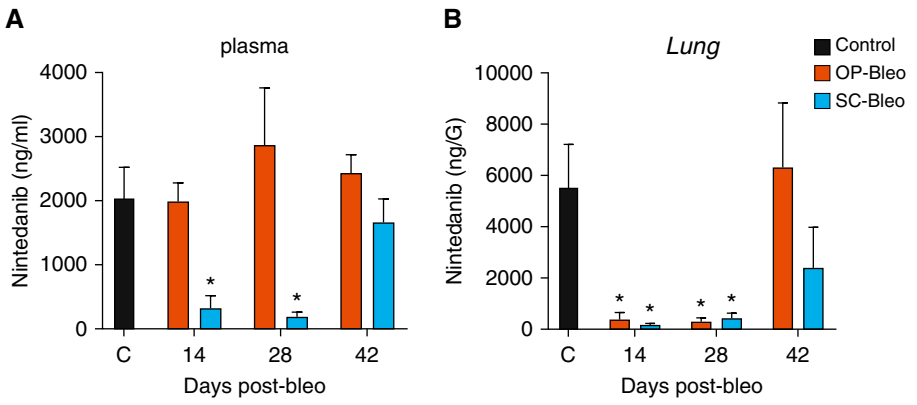

Figure 5. Bleo reduces lung exposure of a P-gp substrate drug, nintedanib. Nintedanib (30 mg/kg) was orally administered to OP-bleo and SC-bleo mice 1 hour before animals were killed, then quantified in (*A*) plasma and (*B*) lung tissue via LC-MS/MS. $n = 4$ mice per group. *$P < 0.05$ indicates significant difference from control group.

We reason that systemic BLM may cause inflammation in the digestive tract, increasing drug transporter activity in the gastrointestinal system with increased expression of P-gp (Figure E5). It is unclear whether there are additional side effects of systemic BLM, which may be misattributed to IPF pathology. Another limitation of the SC-bleo model concerns the age and initial body weight at the time of BLM challenge. IPF is an age-associated disease, and it is known that aged mice are more susceptible to BLM-induced lung fibrosis. Given this age-dependent variability, using mice of different age groups is encouraged in IPF research (2). Here, we show that identical doses of BLM cause significantly different effects on fibrosis grade between 13- and 24-week-old mice due to different starting body weights. This caveat may be another limitation for optimizing the dose for the model between experiments, raising further concern about using this model for preclinical efficacy testing. However, it could still be possible to use these models with a titrated BLM dose to generate fibrosis while reaching comparable target exposure with a test compound in fibrotic lung comparable to that found in control lung. Each preclinical candidate compound might have variable substrate affinity to P-gp or BCRP, so their lung exposure ratios might be different compared with OP-bleo versus control lung. Thus, PK parameters need to be monitored before designing the study to ensure that the drug of interest is on target engagement at intended doses. More broadly, this study underscores the limitation of current animal models used for IPF research, and raises questions about their validity in predicting the clinical outcomes of IPF drugs. A potential solution may be to use MDR1a/b-BCRP knockout mice to generate pulmonary fibrosis using BLM without inducing P-gp and BCRP. Alternatively, promising mouse models are being developed by other groups (34, 35), but the status of ABC transporters has yet to be characterized in these models.

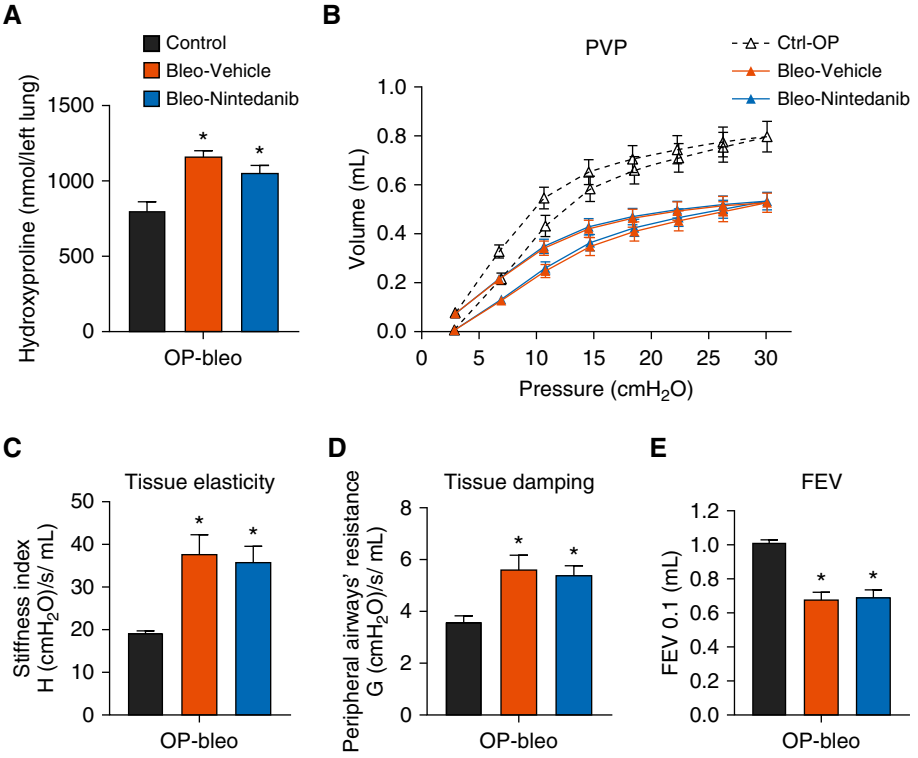

Figure 6. Lack of antifibrotic efficacy of nintedanib in OP-bleo–induced pulmonary fibrosis. (*A*) Hydroxyproline content as fibrosis measurement. (*B*) Pressure–volume curve, (*C*) tissue elasticity, (*D*) tissue damping, and (*E*) FEV as a measure of lung function. $n = 5$ mice per group for control and 7 mice per vehicle and nintedanib-treated groups. *$P < 0.05$ indicates significant difference from vehicle-treated group. Ctrl = control; FEV = forced expiratory volume.

Certain limitations merit mentioning. The IPF lung tissue we examined were obtained from patients after diagnosis and explanted during lung transplantation, so we cannot exclude the possibility that P-gp and BCRP are indeed upregulated at earlier time points in IPF pathogenesis, when acute inflammation and/or acute exacerbation exists. Also, this study focused on only 2 of 48 ABC transporters identified in humans (36), so BLM may induce additional membrane transporters, including those of the solute-carrier family, which were not examined here. Furthermore, P-gp and BCRP may play physiological roles aside from solute efflux. For example, BCRP is a marker of stem and progenitor cells (37) capable of conferring survival advantages under hypoxic conditions

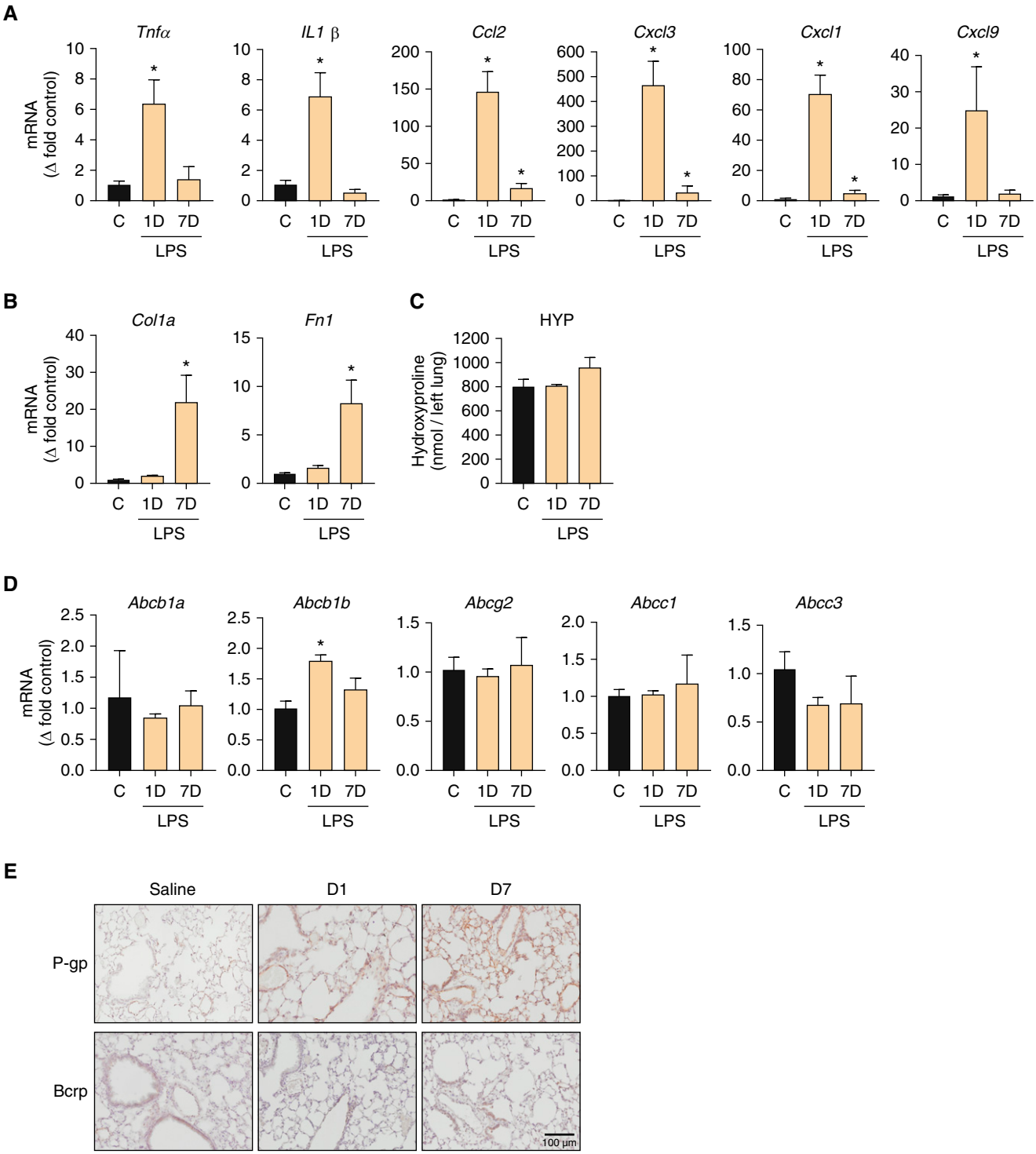

Figure 7. LPS-induced acute lung injury increased P-gp expression, but not BCRP expression, in mice. Gene expression of (*A*) inflammatory cytokines and chemokines and (*B*) fibrogenic markers. (*C*) HYP content. (*D*) Gene expression of drug efflux–associated ABC transporters. (*E*) Protein expression of P-gp and BCRP proteins with immunohistochemistry. Scale bar: 100 μm. $n = 3$ mice per group. $^*P < 0.05$ indicates significant difference from the control group.

(38). In oncology, BCRP is expressed in the nucleus of cancer stem cells, acting as a transcriptional regulator promoting metastasis (39). In this context, an intriguing question is whether BCRP is expressed by progenitor cells in the lungs as part of the wound-healing response, and, if so, whether this mechanism is relevant to IPF. However, it is beyond the scope of this study, which focused on transporter activity and its complications in preclinical efficacy testing.

Although the bleo-induced model has been instrumental to building a framework for understanding IPF pathogenesis, this article identifies a new limitation of this model, and introduces a potential explanation for the attrition of IPF drugs during development. No model may fully reproduce the complexity of human IPF, but addressing limitations to improve them is essential, and will provide more reliable and translatable data about therapeutic targets. We anticipate that this study will facilitate disease model validation, enhance new drug discoveries, and ultimately improve patient outcomes. ■

Author disclosures are available with the text of this article at www.atsjournals.org.

Acknowledgment: The authors thank Ms. Judith Harvey-White (NIH, National Institutes of Alcohol Abuse and Alcoholism) for her technical assistance with liquid chromatography–tandem mass spectrometry experiments.

References

1. Lederer DJ, Martinez FJ. Idiopathic pulmonary fibrosis. *N Engl J Med* 2018;379:797–798.
2. Jenkins RG, Moore BB, Chambers RC, Eickelberg O, Königshoff M, Kolb M, *et al*.; ATS Assembly on Respiratory Cell and Molecular Biology. An Official American Thoracic Society Workshop Report: use of animal models for the preclinical assessment of potential therapies for pulmonary fibrosis. *Am J Respir Cell Mol Biol* 2017;56:667–679.
3. Liu T, De Los Santos FG, Phan SH. The bleomycin model of pulmonary fibrosis. *Methods Mol Biol* 2017;1627:27–42.
4. Adamson IY, Bowden DH. The pathogenesis of bleomycin-induced pulmonary fibrosis in mice. *Am J Pathol* 1974;77:185–197.
5. Tashiro J, Rubio GA, Limper AH, Williams K, Elliot SJ, Ninou I, *et al*. Exploring animal models that resemble idiopathic pulmonary fibrosis. *Front Med (Lausanne)* 2017;4:118.
6. Rees DC, Johnson E, Lewinson O. ABC transporters: the power to change. *Nat Rev Mol Cell Biol* 2009;10:218–227.
7. Thiebaut F, Tsuruo T, Hamada H, Gottesman MM, Pastan I, Willingham MC. Cellular localization of the multidrug-resistance gene product P-glycoprotein in normal human tissues. *Proc Natl Acad Sci USA* 1987;84:7735–7738.
8. Giacomini KM, Huang SM, Tweedie DJ, Benet LZ, Brouwer KL, Chu X, *et al*.; International Transporter Consortium. Membrane transporters in drug development. *Nat Rev Drug Discov* 2010;9:215–236.
9. Gottesman MM, Fojo T, Bates SE. Multidrug resistance in cancer: role of ATP-dependent transporters. *Nat Rev Cancer* 2002;2:48–58.
10. Shanker M, Willcutts D, Roth JA, Ramesh R. Drug resistance in lung cancer. *Lung Cancer (Auckl)* 2010;1:23–36.
11. Kim ES. Chemotherapy resistance in lung cancer. *Adv Exp Med Biol* 2016;893:189–209.
12. Robey RW, Pluchino KM, Hall MD, Fojo AT, Bates SE, Gottesman MM. Revisiting the role of ABC transporters in multidrug-resistant cancer. *Nat Rev Cancer* 2018;18:452–464.
13. El-Chemaly S, Pacheco-Rodriguez G, Malide D, Meza-Carmen V, Kato J, Cui Y, *et al*. Nuclear localization of vascular endothelial growth factor-D and regulation of c-Myc–dependent transcripts in human lung fibroblasts. *Am J Respir Cell Mol Biol* 2014;51:34–42.
14. Ren P, Rosas IO, Macdonald SD, Wu HP, Billings EM, Gochuico BR. Impairment of alveolar macrophage transcription in idiopathic pulmonary fibrosis. *Am J Respir Crit Care Med* 2007;175: 1151–1157.
15. Cullinane AR, Yeager C, Dorward H, Carmona-Rivera C, Wu HP, Moss J, *et al*. Dysregulation of galectin-3: implications for Hermansky-Pudlak syndrome pulmonary fibrosis. *Am J Respir Cell Mol Biol* 2014;50:605–613.
16. Cinar R, Gochuico BR, Iyer MR, Jourdan T, Yokoyama T, Park JK, *et al*. Cannabinoid CB1 receptor overactivity contributes to the pathogenesis of idiopathic pulmonary fibrosis. *JCI Insight* 2017;2: 92281.
17. Egger C, Cannet C, Gérard C, Jarman E, Jarai G, Feige A, *et al*. Administration of bleomycin via the oropharyngeal aspiration route leads to sustained lung fibrosis in mice and rats as quantified by UTE-MRI and histology. *PLoS One* 2013;8:e63432.
18. Lee R, Reese C, Bonner M, Tourkina E, Hajdu Z, Riemer EC, *et al*. Bleomycin delivery by osmotic minipump: similarity to human scleroderma interstitial lung disease. *Am J Physiol Lung Cell Mol Physiol* 2014;306:L736–L748.
19. McGovern TK, Robichaud A, Fereydoonzad L, Schuessler TF, Martin JG. Evaluation of respiratory system mechanics in mice using the forced oscillation technique. *J Vis Exp* 2013;(75):e50172.
20. Devos FC, Maaske A, Robichaud A, Pollaris L, Seys S, Lopez CA, *et al*. Forced expiration measurements in mouse models of obstructive and restrictive lung diseases. *Respir Res* 2017;18:123.
21. Lax S, Wilson MR, Takata M, Thickett DR. Using a non-invasive assessment of lung injury in a murine model of acute lung injury. *BMJ Open Respir Res* 2014;1:e000014.
22. Abe Y, Ohnishi Y, Yoshimura M, Ota E, Ozeki Y, Oshika Y, *et al*. P-glycoprotein-mediated acquired multidrug resistance of human lung cancer cells *in vivo*. *Br J Cancer* 1996;74:1929–1934.
23. Gumbleton M, Al-Jayyoussi G, Crandon-Lewis A, Francombe D, Kreitmeyr K, Morris CJ, *et al*. Spatial expression and functionality of drug transporters in the intact lung: objectives for further research. *Adv Drug Deliv Rev* 2011;63:110–118.
24. Silva R, Carmo H, Vilas-Boas V, Barbosa DJ, Palmeira A, Sousa E, *et al*. Colchicine effect on P-glycoprotein expression and activity: *in silico* and *in vitro* studies. *Chem Biol Interact* 2014;218:50–62.
25. Wollin L, Maillet I, Quesniaux V, Holweg A, Ryffel B. Antifibrotic and anti-inflammatory activity of the tyrosine kinase inhibitor nintedanib in experimental models of lung fibrosis. *J Pharmacol Exp Ther* 2014; 349:209–220.
26. Olson AL, Gifford AH, Inase N, Fernández Pérez ER, Suda T. The epidemiology of idiopathic pulmonary fibrosis and interstitial lung diseases at risk of a progressive-fibrosing phenotype. *Eur Respir Rev* 2018;27:180077.
27. Redente EF, Jacobsen KM, Solomon JJ, Lara AR, Faubel S, Keith RC, *et al*. Age and sex dimorphisms contribute to the severity of bleomycin-induced lung injury and fibrosis. *Am J Physiol Lung Cell Mol Physiol* 2011;301:L510–L518.
28. Cohen AM, Philips FS, Sternberg SS. Studies on the cytotoxicity of bleomycin in the small intestine of the mouse. *Cancer Res* 1972;32: 1293–1300.
29. Braun RK, Ferrick DA, Sterner-Kock A, Kilshaw PJ, Hyde DM, Giri SN. Comparison of two models of bleomycin-induced lung fibrosis in mouse on the level of leucocytes and T cell subpopulations in bronchoalveolar lavage. *Comp Haematol Int* 1996; 6:141–148.
30. Walters DM, Kleeberger SR. Mouse models of bleomycin-induced pulmonary fibrosis. *Curr Protoc Pharmacol* 2008;Chapter 5:Unit 5.46.
31. Liang M, Lv J, Zou L, Yang W, Xiong Y, Chen X, *et al*. A modified murine model of systemic sclerosis: bleomycin given by pump infusion induced skin and pulmonary inflammation and fibrosis. *Lab Invest* 2015;95:342–350.
32. Leslie KO. Idiopathic pulmonary fibrosis may be a disease of recurrent, tractional injury to the periphery of the aging lung: a unifying hypothesis regarding etiology and pathogenesis. *Arch Pathol Lab Med* 2012;136:591–600.
33. Lim MK, Im JG, Ahn JM, Kim JH, Lee SK, Yeon KM, *et al*. Idiopathic pulmonary fibrosis vs. pulmonary involvement of collagen vascular disease: HRCT findings. *J Korean Med Sci* 1997;12:492–498.
34. Nureki SI, Tomer Y, Venosa A, Katzen J, Russo SJ, Jamil S, *et al*. Expression of mutant Sftpc in murine alveolar epithelia drives spontaneous lung fibrosis. *J Clin Invest* 2018;128: 4008–4024.

35. Habiel DM, Espindola MS, Coelho AL, Hogaboam CM. Modeling idiopathic pulmonary fibrosis in humanized severe combined immunodeficient mice. *Am J Pathol* 2018;188:891–903.
36. Dean M, Rzhetsky A, Allikmets R. The human ATP-binding cassette (ABC) transporter superfamily. *Genome Res* 2001;11: 1156–1166.
37. Singh A, Wu H, Zhang P, Happel C, Ma J, Biswal S. Expression of ABCG2 (BCRP) is regulated by Nrf2 in cancer cells that confers side population and chemoresistance phenotype. *Mol Cancer Ther* 2010; 9:2365–2376.
38. Krishnamurthy P, Ross DD, Nakanishi T, Bailey-Dell K, Zhou S, Mercer KE, *et al*. The stem cell marker Bcrp/ABCG2 enhances hypoxic cell survival through interactions with heme. *J Biol Chem* 2004;279: 24218–24225.
39. Liang SC, Yang CY, Tseng JY, Wang HL, Tung CY, Liu HW, *et al*. ABCG2 localizes to the nucleus and modulates CDH1 expression in lung cancer cells. *Neoplasia* 2015;17:265–278.
40. Wishart DS, Feunang YD, Guo AC, Lo EJ, Marcu A, Grant JR, *et al*. DrugBank 5.0: a major update to the DrugBank database for 2018. *Nucleic Acids Res* 2018;46:D1074–D1082.